IRIS AperTO

UNIVERSITÀ DEGLI STUDI DI TORINO

AperTO - Archivio Istituzionale Open Access dell'Università di Torino

Vacuum Thermal Treatments for Surface Engineering of Selective Laser Melted Ti6Al4V Alloy

This is the author's manuscript

Original Citation:

Availability:

This version is available http://hdl.handle.net/2318/1846436 since 2022-03-07T11:08:11Z

Published version:

DOI:10.1007/s11665-021-06046-y

Terms of use:

Open Access

Anyone can freely access the full text of works made available as "Open Access". Works made available under a Creative Commons license can be used according to the terms and conditions of said license. Use of all other works requires consent of the right holder (author or publisher) if not exempted from copyright protection by the applicable law.

(Article begins on next page)

08 February 2025

Vacuum thermal treatments for Surface Engineering of Selective Laser Melted Ti6Al4V alloy

S. Battiston[1, *], F. Montagner[1], V. Zin[1], S. Barison[1], A. Fiorese[2], A. Gionda[2], M. Rancan[3], F. Sordello[4], M. Minella[4], C.A. Biffi[5], J. Fiocchi[5], A. Tuissi[5], L. Armelao[3,6,7]

[1]*Institute of Condensed Matter Chemistry and Technologies for Energy, National Research Council of Italy, ICMATE-CNR, C.so Stati Uniti 4, 35127 Padua, Italy.*

[2]*TAV VACUUM FURNACES SpA; Via dell'Industria 11, 24043 Caravaggio (BG), Italy.*

[3]*Institute of Condensed Matter Chemistry and Technologies for Energy, National Research Council of Italy, ICMATE-CNR, via Marzolo 1, 35131 Padua, Italy.*

[4]*Department of Chemistry and Interdepartmental Centre for Nanostructured Interfaces and Surfaces (NIS), University of Turin, Via P. Giuria 5, 10125 Turin, Italy.*

[5] *Institute of Condensed Matter Chemistry and Technologies for Energy, National Research Council of Italy, ICMATE-CNR, Unit of Lecco, Via Previati 1/E, 23900 Lecco, Italy.*

[6]*Department of Chemical Sciences and Materials Technologies, National Research Council of Italy, Piazzale A. Moro 7, 00185 Rome, Italy.*

[7]*Department of Chemical Sciences, University of Padua, Via Marzolo 1, 35131 Padua, Italy.*

***** *simone.battiston@cnr.it*

Abstract

In the present work, surface engineering of Ti6Al4V, produced via selective laser melting parts was carried out with the aim of investigating how surface features of substrate may improve the coupling with AlTiN coatings deposited by Physical Vapor Deposition

reactive High-Power Impulse Magnetron Sputtering. In particular, the work highlighted how vacuum thermal treatments at 800°C induced peculiar mesoscale morphology and surface chemical modifications of the Ti6Al4V, which contributed to improve the adhesion of the deposited AlTiN thin films. Chemical composition, crystallographic structure, and surface properties of both substrates and coatings were analyzed by Field Emission Scanning Electron Microscopy (equipped with Energy Dispersive Spectroscopy), Atomic Force Microscopy, X-ray Photoelectron Spectroscopy, X-Ray diffraction, nanoindentation, and scratch test measurements.

Keywords: Ti6Al4V, Selective Laser Melting, Additive Manufacturing, Coatings, Films, PVD HiPIMS.

1. INTRODUCTION

Additive manufacturing (AM) is a bottom-up technology that permits the rapid production of components with complex shapes. One of the most well-known advantages of AM consists in supporting the fabrication of components only when and where they are needed, thus reducing or completely eliminating the necessity of forecasting and carrying around them. These aspects are particularly important when the restrictions on mass and volume of the spare parts and tools are critical, as in the case of remote outposts in Antarctica, theatre of military operations, or during long lasting human space missions (Ref 1).

In addition to the actual AM process, a multi-step procedure addressed for ready-to-use tool making should involve post thermal annealing steps, for achieving adequate

mechanical properties of the AMed parts, especially in the case of titanium alloys (Ref 2,3) which possess low ductility values, generally attributed to presence of fine martensitic microstructure (Ref 4–6). For instance, in the case of Ti6Al4V alloy, post-treatments between 480 and 730°C are reported to decrease the residual stresses (Ref 6–8), whilst annealing processes at higher temperatures promote also the martensite decomposition up to overcome the β-transus limit (about 960°C) (Ref 2,4,9).

Further successive processes of AMed ready-to-use tool parts can also regard surface finishing or treatments, as coating processes, which could give improved surface features of the final item (Ref 10,11). From this point of view, the engineering of the interface between the coating and the AMed substrate is fundamental to promote an optimal adhesion and, therefore, the achievement of enhanced surface mechanical properties and protective purposes.

With this aim, this work investigated the effects of vacuum thermal treatments on the interface between AlTiN coatings and Ti6Al4V substrate obtained by Selective Laser Melting (SLM).

Dense AlTiN coatings were deposited by reactive High Power Impulse Magnetron Sputtering (HiPIMS) permitting to successfully coat also substrates exhibiting complex shapes, as AMed tool parts could be. In this case, AlTiN hard coatings represent a good test bench for evaluating how the interface evolution can affect the mechanical features, as hardness or adhesion. In fact, these films are well-known stable systems, widely used in many industrial applications (cutting tools, aircraft engine field, bio-implants, etc..) for their excellent wear and corrosion resistance properties up to 900°C (Ref 12–17).

2. EXPERIMENTAL

Substrates consisted in disks (24 mm in diameter, 5 mm in height) obtained from commercial Ti6Al4V powder (Renishaw) by SLM (model AM400 Renishaw) employing the meander scanning design. The SLM process was carried out under argon atmosphere using power of 200 W, 50 μs of exposure time, 30 μm of layer thickness, 75 μm of point-hatch distance, and platform temperature of 30°C.

The sputtering process was carried out by reactive PVD HiPIMS onto polished Ti6Al4V SLMed substrates using a AlTi target (50:50 at%, 99.9 % pure, with diameter of 50.8 mm, purchased by MaTeck). The base pressure was 5.0×10^{-5} Pa, whilst the working pressure was set at 5.0×10^{-1} Pa with 40 sccm of Ar (99.9997%) and 15 sccm of N_2 (99.998%). The sputtering process was performed by a Ionautics Hipster 6 power supply with constant power density at 15 W cm^{-2}, frequency (1500 Hz), pulse time (50 μs), substrate bias supplied by Ionautics Hipster 1 (-50 V power, frequency 1500 Hz, pulse time 100 μs, synchronized). The substrate temperature was set at 350°C, whilst the substrate-target distance at 60 mm. The sputtering rate was 2.2 μm h^{-1} for a resulting film thickness of 3.7 μm.

The substrate polishing process was carried out with a colloidal silica suspension (OP-U, 0.04 μm, Struers) by using a Tegramin 20 automatic grinder (Struers). Therefore, the substrates were cleaned in acetone and isopropanol in ultrasonic bath, and then dried with N_2 (99.998%).

Both prior and after the coating process, samples were thermal treated with an industrial TAV H3 furnace (40.5 L) at 720°, 800°, and 950°C for 1 h at 10^{-3}-10^{-5} Pa. In particular, the temperatures of the treatments applied to coated samples were selected in order not to

exceed the ones used for treating the corresponding substrates (therefore, if the substate was treated at 800°C, the corresponding coated samples were annealed only at 720 and 800 °C, avoiding the 950°C option). The overall process ended with a free cooling to 350°C, whilst room temperature was reached by 10^5 Pa of Ar inletting.

Three-dimensional topological characterization of surfaces was carried out by a stylus profiler (Bruker, Dektat XT).

The morphology of vacuum thermal treated polished SLMed samples was analyzed by means of Atomic Force Microscopy (AFM) with a Park System XE–100 microscope in contact mode (using Nanosensors PPP-CONTSCR cantilever).

X-ray diffraction (XRD) profiles were collected by a Bragg-Brentano Philips PW 3710 X-Ray diffractometer with a CuKα source (40 kV, 30 mA). An angle of 2° was employed for the thin film analyses in grazing incidence mode. Match! software (version 3.2.1 70) and the inorganic crystal structure database (ICSD) were used for identification of crystallographic phases.

A Sigma Zeiss Field Emission Scanning Electron Microscope (FE-SEM) and an Oxford X-Max Energy Dispersive X-Ray Spectroscopy (EDS) system were used for morphological and compositional characterizations, respectively. The EDS quantitative point analyses of AlTiN films deposited onto monocrystalline doped Si wafers were performed with 20 kV accelerating voltage, with acquisition time of 50 s, collecting data with software INCA 4.14 (Oxford Instruments) and an analytical total within 5 wt%. The software was calibrated for quantification, referencing the standards to Co optimization standard (99.995%, Alpha Aesar USA, purchased by Astimex Standards), with polished

BN (99.99%, Alfa Aesar), as standards for N, and Al (99.999%, Alfa Aesar), Ti (99.99%, Alfa Aesar), and V (obtained by a sputter target 99.9%, Mateck).

X-ray Photoelectron Spectroscopy (XPS) analyses were carried out with a Perkin-Elmer Φ 5600-ci spectrometer using 1486.6 eV Al Kα radiation. The diameter of sample analysis area was set at 800 μm. Survey scans were carried out in the 0−1350 eV range (187.8 eV pass energy, 0.8 eV $step^{-1}$, 0.05 sec $step^{-1}$). Detailed scans were acquired for the C1s, O1s, Al2p, V2p and Ti2p regions (23.5 eV pass energy, 0.1 eV $step^{-1}$, 0.1 sec $step^{-1}$). The error on the binding energy (BE) values was obtained by standard deviation and resulted to be 0.2 eV, whilst the reported atomic composition experimental uncertainty did not overstep ± 5%. The spectrometer was calibrated assuming the BE of the Au $4f_{7/2}$ line at 83.9 eV to the Fermi level. The BE shifts were corrected with respect to the C1s peak of adventitious hydrocarbons at 284.8 eV (Ref 18). Data analysis was performed with a Shirley-type background subtraction, non-linear least-squares curve fitting with Gaussian-Lorentzian peak shapes (Ref 19). The atomic compositions were calculated using peak areas with sensitivity factors provided by Perkin-Elmer, considering the apparatus geometric configuration (Ref 20).

The adhesion of AlTiN coatings deposited onto AMed substrates, polished and then subjected to vacuum thermal treatments, was analysed by UMT-2 tribotester (Bruker) equipped with a standard Rockwell C diamond tip. Test parameters were set following the EN 1071-3 standard for ceramic materials in Progressive Loading Scratch Test (PLST) mode (Ref 21). A minimum of 3 scratch marks were made for each coating to assess the repeatability.

Hardness (H) and elastic modulus (E) values were measured by nanoindentation by means of Nanotest System (Micromaterials, Wrexham, UK) using a Berkovich tip (elastic modulus E=1140 GPa and Poisson ratio ν=0.07). Tests were performed in depth control mode on films deposited onto polished substrates, to suppress the substrate morphology influence. The maximum depth of indents was set within 10% of the mean thickness of coatings, in order to minimize the effect of the substrate mechanical features on the measurements (Ref 22). For a statistical approach, 50 indentations (arranged on square grids) were carried out for each sample. The respective nano-hardness and elastic modulus values were calculated with Oliver and Pharr method applied at the resultant load–displacement curves (Ref 23).

3. RESULTS AND DISCUSSION

3.1 SLMed Ti6Al4V substrate treatments and characterizations

Morphological characterizations of SLMed Ti6Al4V surfaces were carried out by FE-SEM and stylus profilometry, highlighting as SLMed top surface (parallel to the printing plane) was the most suitable to be coated. Indeed, it exhibited a regular topology with low roughness (Ra of 4.2 μm) without prominent asperities (figure 1 a and b), whilst the lateral surfaces were characterized by the presence of non-sintered powder residues, which could interfere with the coating process, as highlighted in figure 1 c. This surface aspect is a typical issue for AMed parts, and the variability of the roughness profile depends on the adopted scanning strategy and part orientations (Ref 24).

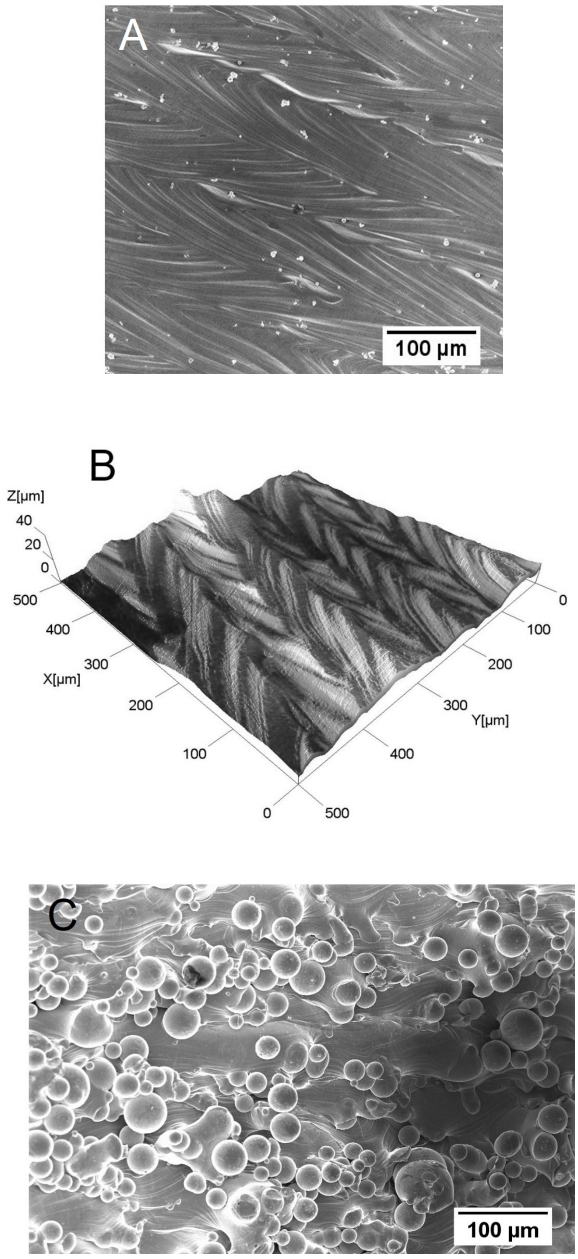

Figure 1: Upper surface secondary electron micrograph (A), upper surface three-dimensional map by stylus profiler *(B), and the lateral surface secondary electron micrograph (C) of samples printed with the meander scanning strategy.*

Vacuum thermal treatments were performed replying those typically carried out for mechanical property improvements of SLMed Ti6Al4V parts (Ref 2,25,26).

In particular, annealing at 720°C and 800°C were aimed to stress reliving (Ref 6–8), whilst 950°C was very close to the β-transus temperature (Ref 2,4,9). The goal of the work was mainly focused on the investigation of how vacuum thermal treatments may affect surface features of SLMed substrates and, consequently, the interface with a functional coating.

According to literature (Ref 27,28), the XRD patterns of Ti6Al4V substrates (figure 2) revealed the typical hexagonal close packed phase peaks (α and α' (Ref 2)), which became sharper along with the temperature treatment increasing, indicating the recrystallization process occurring. After the 950°C treatment, it was possible to observe the presence of low intensity peak related to the incipient decomposition of martensite and the formation of a body-centered cubic β-Ti phase (Ref 29).

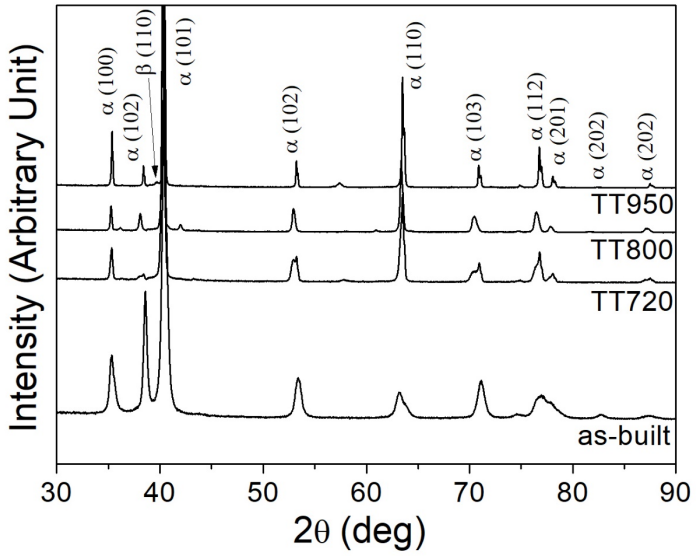

Figure 2: XRD patters of Ti6AlV4 substrates before and after vacuum thermal treatments at 720°, 800°, and 950°C.

Figure 3 listed the FE-SEM surface micrographs of vacuum treated SLMed substrates. The recrystallization process descripted above was particularly evident in the case of 950°C treatments, where large grains could be observed. Nevertheless, the most interesting and unexpected result regarded the changes occurred after the treatment at 800°C, with the formation of a peculiar mesoporous morphology, never reported in literature so far to the best of authors' knowledge.

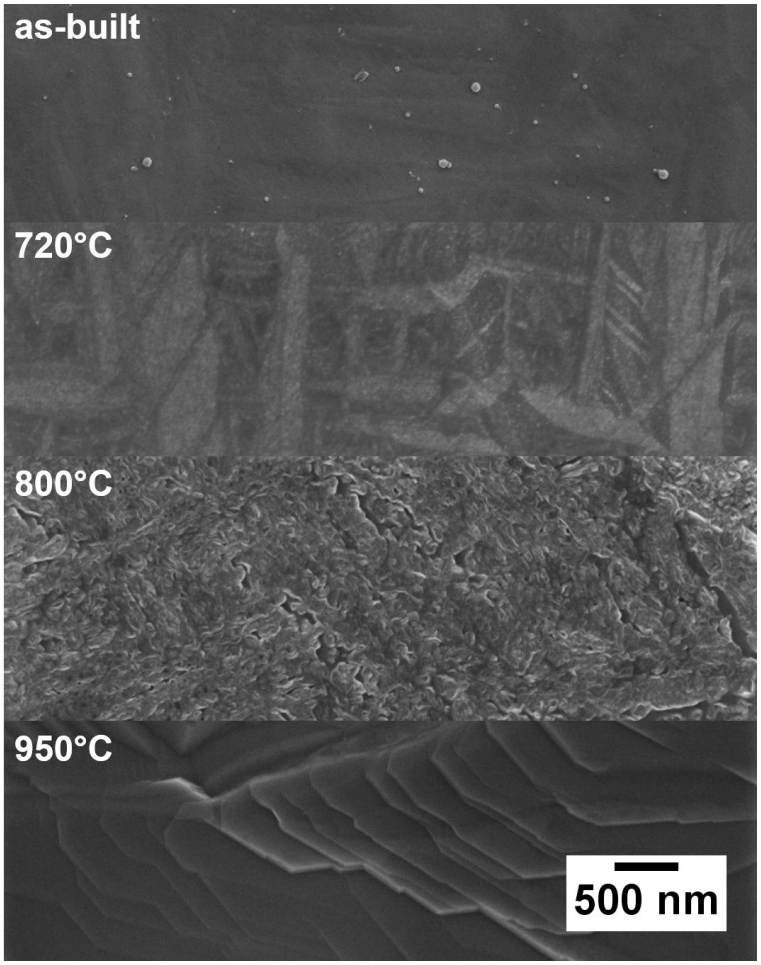

Figure 3: Secondary electron micrographs of the polished SLMed Ti6Al4V samples after several vacuum thermal treatments carried out at different temperatures.

The surface morphology of substrates treated in vacuum at several temperatures and observed by FE-SEM, was confirmed by AFM characterization (figure 4 A, B, and C),

evidencing sample roughness increase with the vacuum thermal treatment temperature. In particular, (Ra) was (6.5±0.9), (10.6±1.0), and (22±3) nm at 95% confidence for the samples treated at 720°, 800°, and 950°C, respectively. The 950°C-treated sample showed significantly larger roughness compared with the samples treated at lower temperatures.

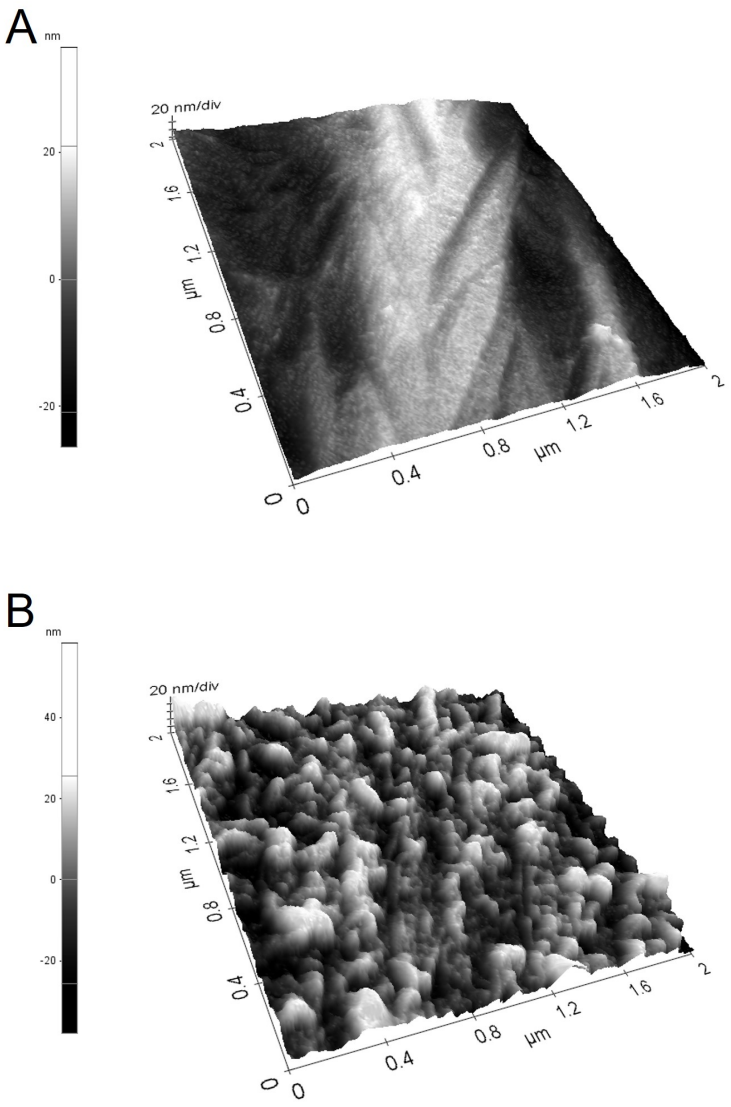

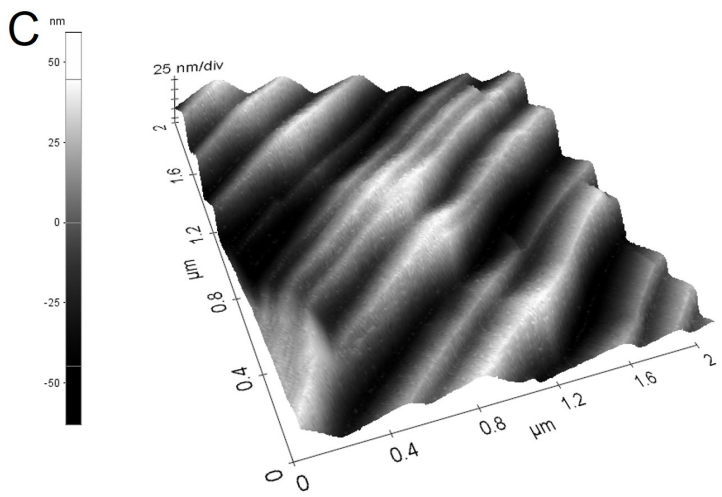

Figure 4: Contact mode AFM maps of sample treated at 720° (A), 800° (B), and 950°C (C).

AFM contact mode measurements highlighted how the lateral force variations were due to surface topological effects and not to friction coefficient changes. Being the trace and retrace very similar, it is reasonable to hypothesize a homogeneous chemical composition along each surface. To assess this feature, XPS measurements were carried out on the different vacuum annealed samples.

XPS analyses, strictly related to the outermost layers of sample surface (typically 3-10 nm), were performed onto unpolished TiAl6V4 substrates treated at 720, 800, and 950°C. They revealed peculiar features associated to the sample vacuum thermal treatment temperatures (for XPS analysis details, see table s1-3, and figures s1 and s2 of the supplementary file). Indeed, it was possible to observe as thermal treatments at higher temperatures induced the formation of carbide species (TiC), likely due to a contamination present in the apparatus, or previously on the samples. The percentage of carbide increased as a function of treatment temperature both in the C1s and Ti2p

regions. At the same time, the oxide contribution in the O1s peak decreased (figure 5), as expected after a vacuum thermal treatment.

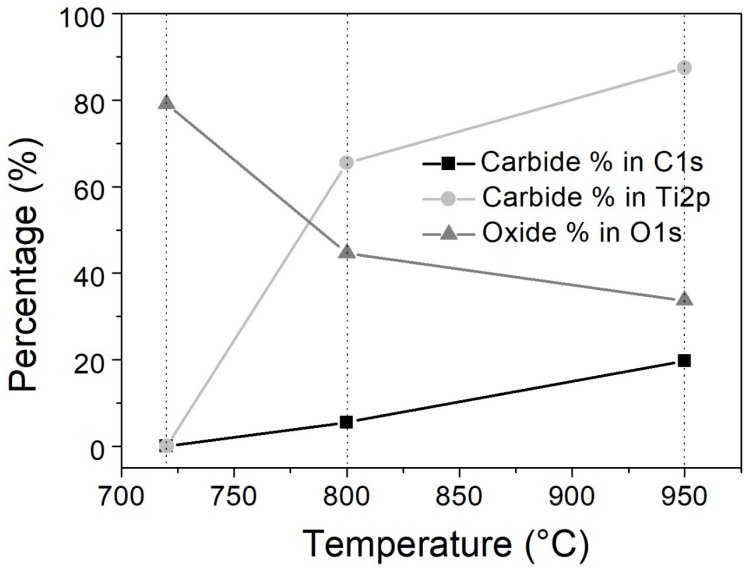

Figure 5: Percentage of carbide contribution in C1s and Ti2p XPS regions and of oxide contribution in the O1s region for unpolished samples treated at 720°, 800°, and 950°C.

3.2 AlTiN thin film characterizations

With the aim of investigating how surface substrate features may affect the properties of functional coatings, AlTiN films were deposited by reactive HiPIMS. Figure 6 shows the typical columnar dense morphology of coatings. EDS quantitative analyses confirmed the stoichiometry of $Al_{0.5}Ti_{0.5}N_{1.0}$.

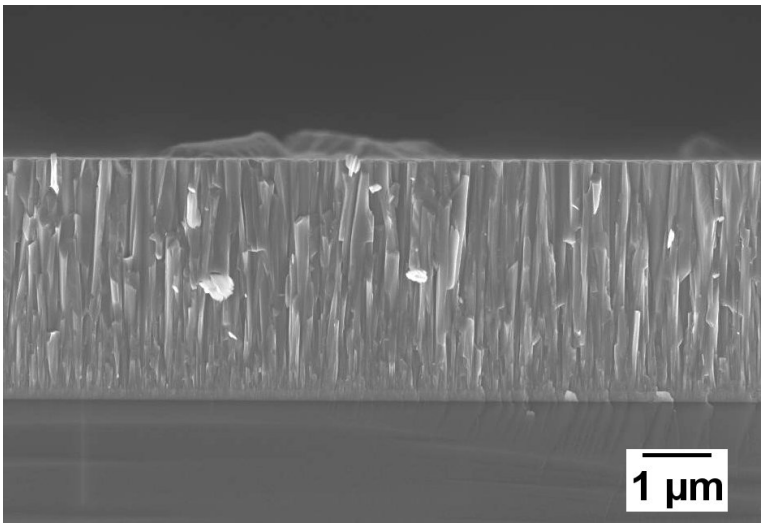

Figure 6: Secondary electron micrograph of AlTiN thin film deposited onto Si.

Despite the mesoscale surface morphology of substrates changed as a function of the treatment temperature, it did not seem to particularly affect growth of AlTiN films, which, unlike the underlying materials, showed unaltered surface morphologies (figure 7).

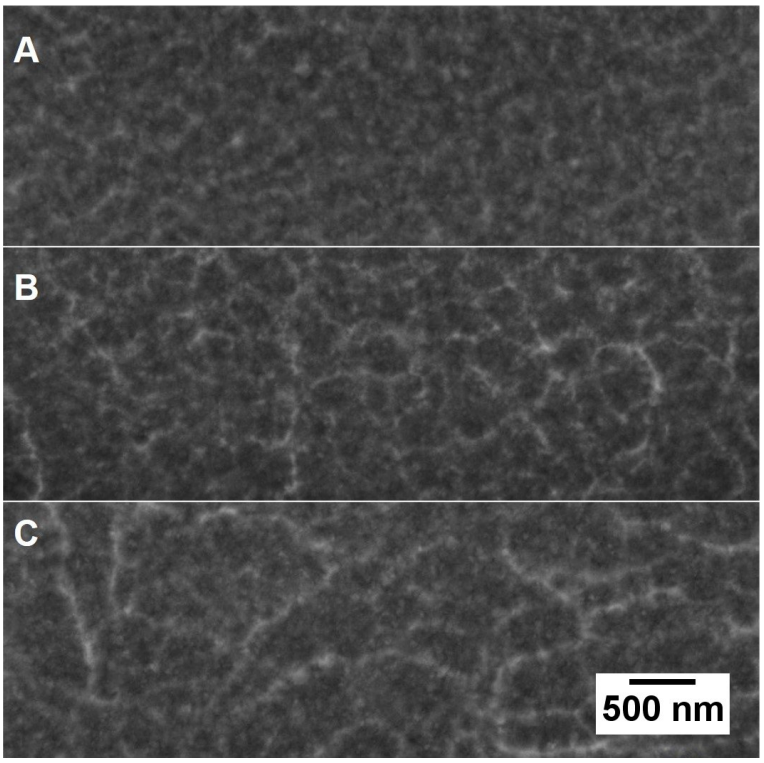

Figure 7: Secondary electron micrographs of the AlTiN thin films deposited onto unpolished SLMed Ti6Al4V substrates previously vacuum thermal treated at 720°C (A), 800°C (B), and 950°C (C).

On the other hand, figure 8 shows as the AlTiN films perfectly fitted the complex tridimensional topology of the substrates, confirming HiPIMS as the suitable choice for coating AMed tool parts.

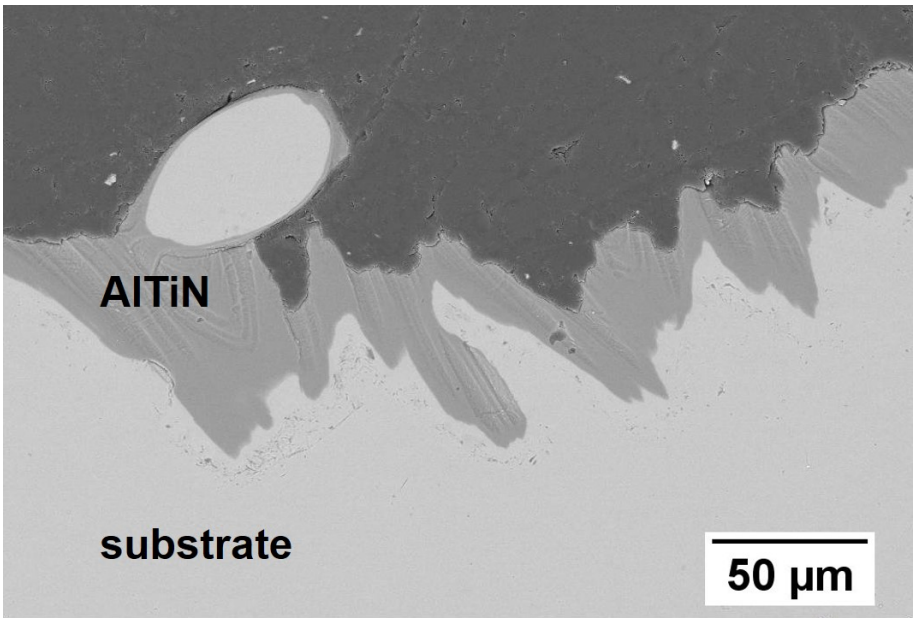

Figure 8: Backscattered electron micrograph of tilted cross section of the AlTiN thin film deposited onto unpolished SLMed Ti6Al4V substrates.

In order of investigating how the peculiar surface mesoscale morphologies of the Ti6Al4V, obtained after the several vacuum treatments, may affect the coating adhesion, scratch test measurements were carried out.

Polished Ti6Al4V surfaces were vacuum treated at 720°, 800°, 950°C prior of the coating process, with the aim of obtaining planar surfaces with different mesoscale morphologies. Then, AlTiN films were deposited.

During a scratch test, while moving along the sample surface, the tip induces specific damages of the coating, especially cracks or delamination, occurring at typical values for the applied load, denoted as critical loads Lc. The first failure Lc1 corresponds to initial cracking, with formation of circular cracks paralleling with the indenter. The second failure Lc2 corresponds to extensive cracking, generally radial cracks formed at the film/substrate interface due to the film bending. Final failure Lc3 coincides with

delamination of the coating from the substrate. Lc3 value for the three different coatings were identified comparing the scratch surface micrographs to the friction force and the acoustic emission collected data as a function of the track length (an example is listed in figure s3 of supplementary file).

The scratch tracks, illustrated in Figure 9 showed that brittle failure occurred in all AlTiN coatings with consequent substrate exposure, even outside the scratch track (Ref 30). The best performing coating, in terms of film delamination, was the one deposited onto the substrate treated at 800°C, exhibiting a critical load Lc3 of (61.0±3.0) N. Conversely, films with substrates vacuum treated at 720° and 950°C showed lower Lc3 values of (53.0±2.6) N, and (45.0±2.2) N, respectively.

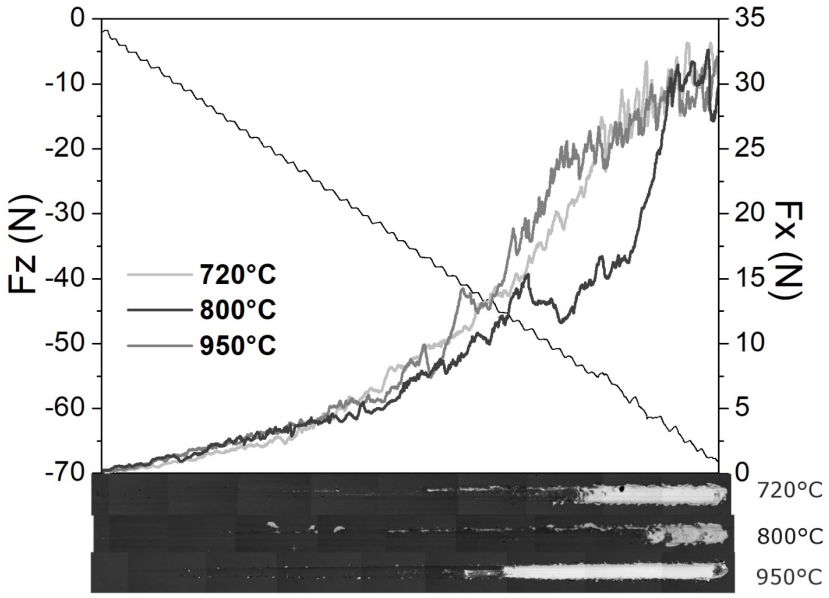

Figure 9: Scratch test curves of the AlTiN films deposited onto vacuum thermal treated SLMed substrates, where Fx (friction force) and Fz (applied load) were reported as functions of displacement.

Not only the mean surface roughness of samples, but also the surface morphology played an important role in this behaviour. Indeed, in addition to the roughness value of the substrate treated at 800°C, almost halfway between 720°C and 950°C, a peculiar homogeneous structured surface morphology was observed for that sample. This feature affected the adhesion, leading to its enhancing.

Conversely, higher roughness values, as in the case of substrate treated at 950°C, led to a lower film adhesion with early-onset complete delamination without earlier cracking (visible in the detail in Figure s3 of supplementary file). In general, an excessive roughness can be responsible for defects presence within the growing film, with the consequent formation of a less stable film/substrate interface, combined with coating delamination in the stress concentrated zones, located at highest peak points of sample surfaces (Ref 31).

Unfortunately, observing the scratch tests only, it was very difficult to separate the contribution to the coating/substrate adhesion given by the surface roughness and the physical/structural properties of the substrate, since the polishing operation affects and modifies the mechanical properties of the surface, as well as the roughness.

Mechanical characterization of the films deposited onto polished substrates were performed to verify if substrate mechanical and microstructural properties could affect the final properties of deposited coatings. Since nanoindentation is strongly sensitive to surface topology, it was necessary to avoid any difference between the several surface morphologies of substrates, to make comparable measures among different samples. For this reason, surface polishing operation was applied to substrates after the thermal treatments, and prior to the coating process.

The measurements were carried out on film deposited onto vacuum treated substrates and even on film subjected to further vacuum treatments, as listed in the following table (table1).

Table 1: AlTiN film deposited onto polished substrates the respective vacuum thermal treatments.

Sample name	**Substrate vacuum thermal treatment prior to the polishing**	**Sample vacuum thermal treatment after the coating**
sub+film+TT720	-	720°C
sub+film+TT800	-	800°C
sub+TT720+film+TT720	720°C	720°C
sub+TT800+film	800°C	-
sub+TT800+film+TT720	800°C	720°C
sub+TT800+film+TT800	800°C	800°C
sub+TT950+film	950°C	-
sub+TT950+film+TT720	950°C	720°C
sub+TT950+film+ TT800	950°C	800°C

The nanoindentation results (Figure 10) did not highlight a clear trend neither marked variations among the several combinations of vacuum treatments, and all values resulted comparable within the experimental errors. Nevertheless, it was possible to observe as deposited nitride coatings exhibited a very good mechanical stability at high temperatures and were suitable to perform an effective protective function towards the underlying

substrates. In fact, no loss or deterioration of mechanical properties was observed following exposure of the samples to heat treatments. The sole limit to the vacuum thermal treatments was related to the film cracking occurred when coated samples were treated at 950°C. It was likely due to the Ti6Al4V substrate recrystallization phenomenon which occurred at such temperature. The consequent detrimental cell/volume expansion of the material led to the coating failure for geometrical mismatching with films.

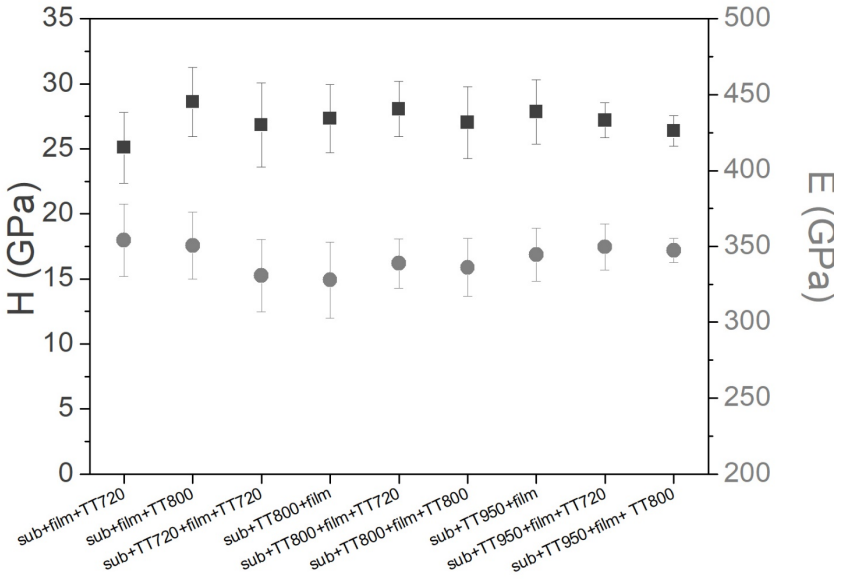

Figure 10: Hardness (H) and Elastic modulus (E) of AlTiN thin films deposited onto vacuum thermal treated, and the polished, SLMed substrates (for sample names, see table 1).

A further demonstration of AlTiN coating stability at high temperature without downgrading its properties also came by from the substantially unaltered film morphology and XRD profiles after the several vacuum thermal treatments (figure S4 and S5 of supplementary file, respectively). In addition to its well-known tribological

performances, the AlTiN material stability was actually the main reason for why it was chosen as the coating material in this study (Ref 12–16).

CONCLUSIONS

The study demonstrated that the upper complex tridimensional surface of the SLMed samples can be successfully coated by reactive PVD HiPIMS, improving the surface features of potential AMed tool parts. Exploiting the typical vacuum thermal treatment process at industrial scale for mechanical property improvement of TiAl6V4 SLMed parts, a novel peculiar surface mesoscale morphology of Ti6Al4V substrate was observed after vacuum thermal treatments carried out at 800°C. In case of coating the material for protective purposes, this feature demonstrated to be the most suitable, since it contributed to improve thin film adhesion. Moreover, AlTiN material resulted to be an appropriate coating for Ti6Al4V AMed tool parts. In fact, it was able to maintain substantially unaltered its mechanical properties, even in case of further vacuum thermal treatments below 950°, temperature at which coating breaking can occur due to substrate recrystallization phenomena and resulting geometric mismatch.

ACKNOWLEDGMENTS

The authors are grateful to Matteo Leder for the valuable support on relationships with companies. This work has been funded by TAV VACUUM FURNACES SpA and by the National Research Council of Italy - Ministry of Economic Development (Italy) Agreement 2019 – 2021 “Ricerca di Sistema Elettrico Nazionale”.

References:

1. T. Prater, N. Werkheiser, F. Ledbetter, D. Timucin, K. Wheeler, and M. Snyder, 3D Printing in Zero G Technology Demonstration Mission: Complete Experimental Results and Summary of Related Material Modeling Efforts, *Int. J. Adv. Manuf. Technol.*, 2019, **101**(1–4), p 391–417.

2. C. Lora, A. Fiorese, G. Rossato, A. Jam, and M. Pellizzari, Properties of Additive Manufactured Ti6Al4V after Different Vacuum Heat Treatments, *Euro PM 2019 Congress and Exhibition*, 2020.

3. B. Vrancken, L. Thijs, J.P. Kruth, and J. Van Humbeeck, Heat Treatment of Ti6Al4V Produced by Selective Laser Melting: Microstructure and Mechanical Properties, *J. Alloys Compd.*, 2012, **541**, p 177–185.

4. S. Cao, R. Chu, X. Zhou, K. Yang, Q. Jia, C.V.S. Lim, A. Huang, and X. Wu, Role of Martensite Decomposition in Tensile Properties of Selective Laser Melted Ti-6Al-4V, *J. Alloys Compd.*, Elsevier Ltd, 2018, **744**, p 357–363.

5. B. Vrancken, L. Thijs, J.P. Kruth, and J. Van Humbeeck, Heat Treatment of Ti6Al4V Produced by Selective Laser Melting: Microstructure and Mechanical Properties, *J. Alloys Compd.*, Elsevier, 2012, **541**, p 177–185.

6. T. Vilaro, C. Colin, and J.D. Bartout, As-Fabricated and Heat-Treated Microstructures of the Ti-6Al-4V Alloy Processed by Selective Laser Melting, *Metall. Mater. Trans. A Phys. Metall. Mater. Sci.*, Springer, 2011, **42**(10), p 3190–3199.

7. M.J. Donachie, Titanium: A Technical Guide, ASM international, 2000.

8. M. Simonelli, Y.Y. Tse, and C. Tuck, Effect of the Build Orientation on the Mechanical Properties and Fracture Modes of SLM Ti-6Al-4V, *Mater. Sci. Eng. A*, Elsevier Ltd, 2014, **616**, p 1–11.

9. W. Xu, E.W. Lui, A. Pateras, M. Qian, and M. Brandt, In Situ Tailoring Microstructure in Additively Manufactured Ti-6Al-4V for Superior Mechanical Performance, *Acta Mater.*, Elsevier Ltd, 2017, **125**, p 390–400.

10. S. Yao and T. Wang, Improved Surface of Additive Manufactured Products by Coating, *J. Manuf. Process.*, 2016, **24**, p 212–216.

11. D.G. Agredo Diaz, A. Barba Pingarrón, J.J. Olaya Florez, J.R. González Parra, J. Cervantes Cabello, I. Angarita Moncaleano, A. Covelo Villar, and M.Á. Hernández Gallegos, Evaluation of the Corrosion Resistance of a Ni-P Coating Deposited on Additive Manufacturing Steel: A Dataset, *Data Br.*, Elsevier Inc., 2020, **32**, p 106159.

12. E. Schäffer and G. Kleer, Mechanical Behavior of (Ti,Al)N Coatings Exposed to Elevated Temperatures and an Oxidative Environment, *Surf. Coatings Technol.*, 2000, **133**–**134**(134), p 215–219.

13. K. Chakrabarti, J.J. Jeong, S.K. Hwang, Y.C. Yoo, and C.M. Lee, Effects of Nitrogen Flow Rates on the Growth Morphology of TiAlN Films Prepared by an Rf-Reactive Sputtering Technique, *Thin Solid Films*, 2002, **406**, p 159–163.

14. R. Gago, F. Soldera, R. Hübner, J. Lehmann, F. Munnik, L. Vázquez, A. Redondo-Cubero, and J.L. Endrino, X-Ray Absorption near-Edge Structure of Hexagonal Ternary Phases in Sputter-Deposited TiAlN Films, *J. Alloys Compd.*, 2013, **561**, p

87–94.

15. B. Subramanian, C. V. Muraleedharan, R. Ananthakumar, and M. Jayachandran, A Comparative Study of Titanium Nitride (TiN), Titanium Oxy Nitride (TiON) and Titanium Aluminum Nitride (TiAlN), as Surface Coatings for Bio Implants, *Surf. Coatings Technol.*, 2011, **205**(21–22), p 5014–5020.

16. S. Battiston, F. Montagner, S. Fiameni, A. Famengo, S. Boldrini, A. Ferrario, C. Fanciulli, F. Agresti, and M. Fabrizio, AlTiN Based Thin Films for Degradation Protection of Tetrahedrite Thermoelectric Material, *J. Alloys Compd.*, Elsevier, 2019, **792**, p 953–959.

17. S.M. Deambrosis, F. Montagner, V. Zin, M. Fabrizio, C. Badini, E. Padovano, M. Sebastiani, E. Bemporad, K. Brunelli, and E. Miorin, Ti1−xAlxN Coatings by Reactive High Power Impulse Magnetron Sputtering: Film/Substrate Interface Effect on Residual Stress and High Temperature Oxidation, *Surf. Coatings Technol.*, Elsevier, 2018, **354**, p 56–65.

18. D. Briggs and M. Seah, "In Practical Surface Analysis," Wiley, Ed., Wiley: Chichester, UK, 1990.

19. D.A. Shirley, High-Resolution x-Ray Photoemission Spectrum of the Valence Bands of Gold, *Phys. Rev. B*, APS, 1972, **5**(12), p 4709–4714.

20. J.F. Moulder, W.F. Stickle, P.E. Sobol, and K.D. Bomben, Handbook of X-Ray Photoelectron Spectroscopy, Chastain J. Physical Electronics Industries, Ed., Eden Prairie, MN, 1992.

21. UNI EN 1071-3: 2005 Advanced Technical Ceramics-Methods of Test for

Ceramic Coatings-Part 3: Determination of Adhesion and Other Mechanical Failure Modes by a Scratch Test.

22. A.M. Korsunsky, M.R. McGurk, S.J. Bull, and T.F. Page, On the Hardness of Coated Systems, *Surf. Coatings Technol.*, Elsevier, 1998, **99**(1–2), p 171–183.

23. W.C. Oliver and G.M. Pharr, An Improved Technique for Determining Hardness and Elastic Modulus Using Load and Displacement Sensing Indentation Experiments, *J. Mater. Res.*, Cambridge University Press, 1992, **7**(6), p 1564–1583.

24. C.A. Biffi, J. Fiocchi, E. Ferrario, A. Fornaci, M. Riccio, M. Romeo, and A. Tuissi, Effects of the Scanning Strategy on the Microstructure and Mechanical Properties of a TiAl6V4 Alloy Produced by Electron Beam Additive Manufacturing, *Int. J. Adv. Manuf. Technol.*, Springer, 2020, **107**, p 4913–4924.

25. Z. Fan and H. Feng, Study on Selective Laser Melting and Heat Treatment of Ti-6Al-4V Alloy, *Results Phys.*, Elsevier B.V., 2018, **10**, p 660–664.

26. J. Fiocchi, C.A. Biffi, D. Scaccabarozzi, B. Saggin, and A. Tuissi, Enhancement of the Damping Behavior of Ti6Al4V Alloy through the Use of Trabecular Structure Produced by Selective Laser Melting, *Adv. Eng. Mater.*, Wiley Online Library, 2020, **22**(2), p 1900722.

27. B. Wysocki, P. Maj, R. Sitek, J. Buhagiar, K.J. Kurzydłowski, and W. Świeszkowski, Laser and Electron Beam Additive Manufacturing Methods of Fabricating Titanium Bone Implants, *Appl. Sci.*, 2017, **7**(7), p 657.

28. J. He, D. Li, W. Jiang, L. Ke, G. Qin, Y. Ye, Q. Qin, and D. Qiu, The Martensitic

Transformation and Mechanical Properties of Ti6Al4V Prepared via Selective Laser Melting, *Materials (Basel)*, 2019, **12**(2).

29. D. Banerjee and J.C. Williams, Perspectives on Titanium Science and Technology, *Acta Mater.*, Pergamon, 2013, **61**(3), p 844–879.

30. S.J. Bull, Failure Modes in Scratch Adhesion Testing, *Surf. Coatings Technol.*, 1991, **50**(1), p 25–32.

31. J. Takadoum and H.H. Bennani, Influence of Substrate Roughness and Coating Thickness on Adhesion, Friction and Wear of TiN Films, *Surf. Coatings Technol.*, Elsevier, 1997, **96**(2–3), p 272–282.